Comparison of liquid sloshing in different tanks based on MPS method

Fengze Xie, Xiang Chen, Decheng Wan*

State Key Laboratory of Ocean Engineering, School of Naval Architecture Ocean and Civil Engineering, Shanghai Jiao Tong University, Collaborative Innovation Center for Advanced Ship and Deep-Sea Exploration, Shanghai 200240, China

*Corresponding author: dcwan@sjtu.edu.cn

Abstract

The selection of tanks' shape may affect its life-span and safety because different shape tanks show different sensitivity to liquid sloshing. In this paper, responses of different shape tanks under external excitation are compared. The in-house solver MLParticle-SJTU solver based on moving particle semi-implicit method is employed for the simulation. The convergent validation is conducted to verify the reliability of present solver to simulate the sloshing in cylindrical tank. Sloshing in the rectangular tank and cylindrical tank with different filling ratios is simulated. The characteristics of flow field and pressure time history are presented. In addition, Three-dimensional effect can be observed in simulation, which have great influence on the sloshing and the load applied on the wall.

Keywords: Moving particle semi-implicit method; Liquid sloshing; MLParticle-SJTU solver; Three-dimensional effect

Introduction

Due to the uneven distribution of energy in different region, a large amount of energy needs to be transported from one area to another every year. Liquid sloshing is a significant issue in the transportation of liquefied natural gas, oil and liquefied petroleum gas. The liquid inside a partially filled tank will be induced to violent oscillations and large impact pressure on the tank under external excitations which are large amplitude or resonance frequency of sloshing. Therefore, many researchers have investigated the characters and mechanisms of sloshing.

There are many methods to investigated sloshing problem. Compared with other traditional methods, Computational Fluid Dynamic (CFD) technology has some extra advantages. It can provide more detailed flow field information, which facilitate people to analyze the evolution process of sloshing fluid flow field, discover the physical mechanism behind sloshing phenomenon, and provide guidance for experiment. This is the reason why more researchers focus their attention on CFD technology. Faltisnen (1978) firstly applied Boundary-Element-Method (BEM) to investigate the sloshing problem [1]. Milkelis et al. (1984) used the Marker-And-Cell (MAC) method to capture the free surface and simulate the 2-D liquid sloshing in a rectangular tank and a membrane tank [2]. Liu et al. (1994) adopted Arbitrary-Lagrangian-Euler (ALE) to capture the free surface and simulate the large -amplitude sloshing [4]. Sussman (1998) studied the 2-D liquid sloshing based on the modified Level-set method, which can simulate complex free surface deformation successfully [3]. Kim et al. (2001) applied the Finite-Difference-Method (FDM) and Impulse-Response-Function (IRF) method to study the coupling effects of ship motion and sloshing [5]. Belakroum et al. (2010) used Finite-Element-Method (FEM) to simulate the sloshing of rectangular tank and proposed a new method to reduce sloshing [6]. Zhuang et al. (2016) used the naoe-FOAM-SJTU solver based

on Finite-Volume-Method (FVM) to conduct the numerical simulation of FPSO motion coupled with LNG sloshing [7].

Particle method has the superiority to handle the problem of large deformation of free surface, which is proven to be valid and efficient in simulating liquid sloshing in previous work. Iglesias et al. (2004, 2006) used Smoothed Particle Hydrodynamics (SPH) method to simulate the sloshing in the anti-rolling tank of a fishing vessel [8] [9]. Delorme et al. (2009) used SPH method to investigate the impact pressure in the case of shallow water sloshing. Zhang et al. (2012) used Moving Particle Semi-implicit method to simulate liquid sloshing in LNG tank [11]. Koh et al. (2013) adopted Consistent Particle Method (CPM) to investigate the sloshing problem of a rectangular tank with constrained floating baffles under sway excitation [12]. Zhang et al. (2017) applied MPS method and FEM method to study the liquid sloshing in rectangular tank with elastic bulkhead [13]. Chen et al. (2017) introduced the GPU technology to MPS method to accelerate the simulation in 3-D sloshing [14]. Wen et al. (2018) simulate the three-layer-liquid sloshing in the rigid tank with multiphase MPS method [15].

In this study, an in-house solver MLParticle-SJTU based on modified MPS is employed to simulate the three-dimensional sloshing. In the first section, the description of modified MPS method is presented briefly. In the second section, the convergent validation is carried out to verify the accuracy of present solver in the simulation of cylindrical tank and the simulation result shows good agreements with experimental data. Then, the sloshing in three-dimensional cylindrical tank and rectangular tank with different filling ratios is simulated at their respective natural frequencies. The slamming pressure in different location is measured and the comparison of those two type tanks is conducted.

Numerical Method

MPS method is proposed by Koshizuka et al. (1996) for viscous incompressible fluid [16]. In this section, basic theories and discretization process of MPS will be presented in detail.

Governing Equations

The governing equations contain continuity equation and Navier-Stokes equation.

$$\nabla \cdot \vec{V} = 0 \tag{1}$$

$$\frac{D\vec{V}}{Dt} = -\frac{1}{\rho}\nabla P + \nu\nabla^2\vec{V} + \vec{g} \tag{2}$$

Where the $\vec{V}$ is the velocity vector, the t is the time, the ρ is the fluid density, P is the pressure, ν is the kinematic viscosity, $\vec{g}$ is the gravity acceleration vector.

Kernel Function

In MPS method, the interaction between particles is controlled by kernel function, which plays a role of weight function in the discretization process. In order to avoid non-physical pressure oscillation, the kernel function presented by Zhang et al. (2014) is employed here [17].

$$W(r)=\begin{cases}\dfrac{r_e}{0.85r+0.15r_e}-1 & 0\le r<r_e\\ 0 & r_e\le r\end{cases} \tag{3}$$

Where r is the distance between two particles and r_e is the radius of the particle interaction.

Gradient Model

The gradient vector of particle i is the weighted average of the gradient vectors between particle i and all its neighboring particles j. The model adopted in this paper is proposed by Tanaka et al. (2010), which meets the law of conservation of momentum.

$$<\nabla\phi>_i=\frac{d}{n^0}\sum_{j\neq i}\frac{\phi_j+\phi_i}{|\vec{r}_j-\vec{r}_i|^2}(\vec{r}_j-\vec{r}_i)\cdot W(|\vec{r}_j-\vec{r}_i|) \tag{4}$$

Where ϕ is a physical quantity, d is the number of space dimension, n^0 is the initial particle density, $\vec{r}$ is the position vector relative to origin.

Laplacian Model

The Laplacian model is the weighted average of the distribution of a quantity ϕ from particle i to neighboring particle j, which is needed in the solution of viscosity term of N-S equation and the space discretization of Pressure Poisson Equation.

$$<\nabla^2\phi>_i=\frac{2d}{n^0\lambda}\sum_{j\neq i}(\phi_j-\phi_i)\cdot W(|\vec{r}_j-\vec{r}_i|) \tag{5}$$

$$\lambda=\frac{\sum_{j\neq i}W(|\vec{r}_j-\vec{r}_i|)\cdot|\vec{r}_j-\vec{r}_i|^2}{\sum_{j\neq i}W(|\vec{r}_j-\vec{r}_i|)} \tag{6}$$

Pressure Poisson Equation （*PPE*)

In MPS method, the acquirement of pressure is through solving PPE. In this paper, mixed source term method is used to solve PPE, which is developed by Tanaka et al. (2010) [18].

$$<\nabla^2P^{k+1}>_i=(1-\gamma)\frac{\rho}{\Delta t}\nabla\cdot\vec{V}_i^*-\gamma\frac{\rho}{\Delta t^2}\frac{<n^*>_i-n^0}{n^0} \tag{7}$$

Where P^{k+1} is the pressure of the step $k+1$, γ is a blending parameter, Δt is the time step, $\vec{V}_i^*$ is the temporal velocity, n^* is the temporal particle density. In this paper, the value of γ set to be 0.01.

Divergence Model

Divergence model is similar to the gradient model and it is used to discrete velocity divergence in the PPE.

$$\nabla \cdot \vec{V} = \frac{d}{n^0} \sum_{j \neq i} \frac{\left(\vec{r}_j - \vec{r}_i\right) \cdot \left(\vec{V}_j - \vec{V}_i\right)}{\left|\vec{r}_j - \vec{r}_i\right|^2} W\left(\left|\vec{r}_j - \vec{r}_i\right|\right) \tag{8}$$

Free Surface Detection

An improved surface particle detection method developed by Zhang et al. (2010) is adopted in this paper [19], which can distinguish the particles of free surface from the others efficiently. This approach is based on the asymmetry distribution of neighboring particles.

$$< n >_i^* \ < \beta n^0 \tag{9}$$

$$< \vec{F} >_i = \frac{d}{n^0} \sum_{j \neq i} \frac{1}{|\vec{r}_i - \vec{r}_j|} (\vec{r}_i - \vec{r}_j) W\left(\left|\vec{r}_j - \vec{r}_i\right|\right) \tag{10}$$

$$< |\vec{F}| >_i \ > \alpha |\vec{F}_0| \tag{11}$$

Where β and α are parameters, $\vec{F}$ is a vector which represents the asymmetry distribution of neighboring particles. When $\beta \leq 0.8$ or $\beta \geq 0.97$, the type of particles can be set to free surface. When the $0.8 < \beta < 0.97$, formulas (9) and (10) are used to judge free surface particles. The value of α is set to be 0.9.

Boundary Condition

There are multilayer particles arranged at the solid boundary. One layer of wall particles is arranged near the fluid particles and their pressure is solved by PPE. Two layers of ghost particles are configured because fluid particles lack neighbor particles on the side of the solid wall. The pressure of ghost particles is obtained by extrapolation. Both the wall particles and the ghost particles don't update their velocity and displacement after they gain the pressure.

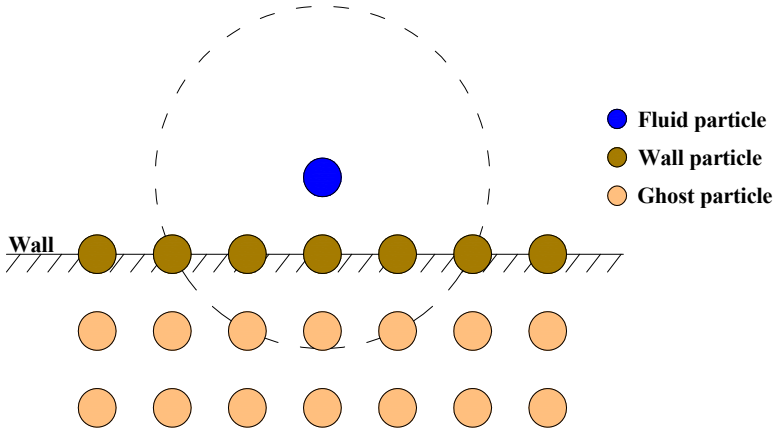

Figure 1. Diagram of boundary particles

Numerical Simulations

In this section, the responses of a cylindrical tank and a rectangular tank under external

excitation are compared. The cylindrical tank comes from the experiment conducted by Kobayashi et al. (1986) [20]. The parameters of the rectangular tank are selected according to the cylindrical tank and its cross-sectional area is a square. Figure 2 shows the geometry of those two liquid tanks. The dimensions of tanks are 0.94m (L), 0.47m (D), 0.47m (B) and 0.47m (H). Those two liquid tanks sway harmonically under the external excitation.

$$x = A\sin(\omega t) \tag{12}$$

Where A is the amplitude of motion, ω is the excitation frequency.

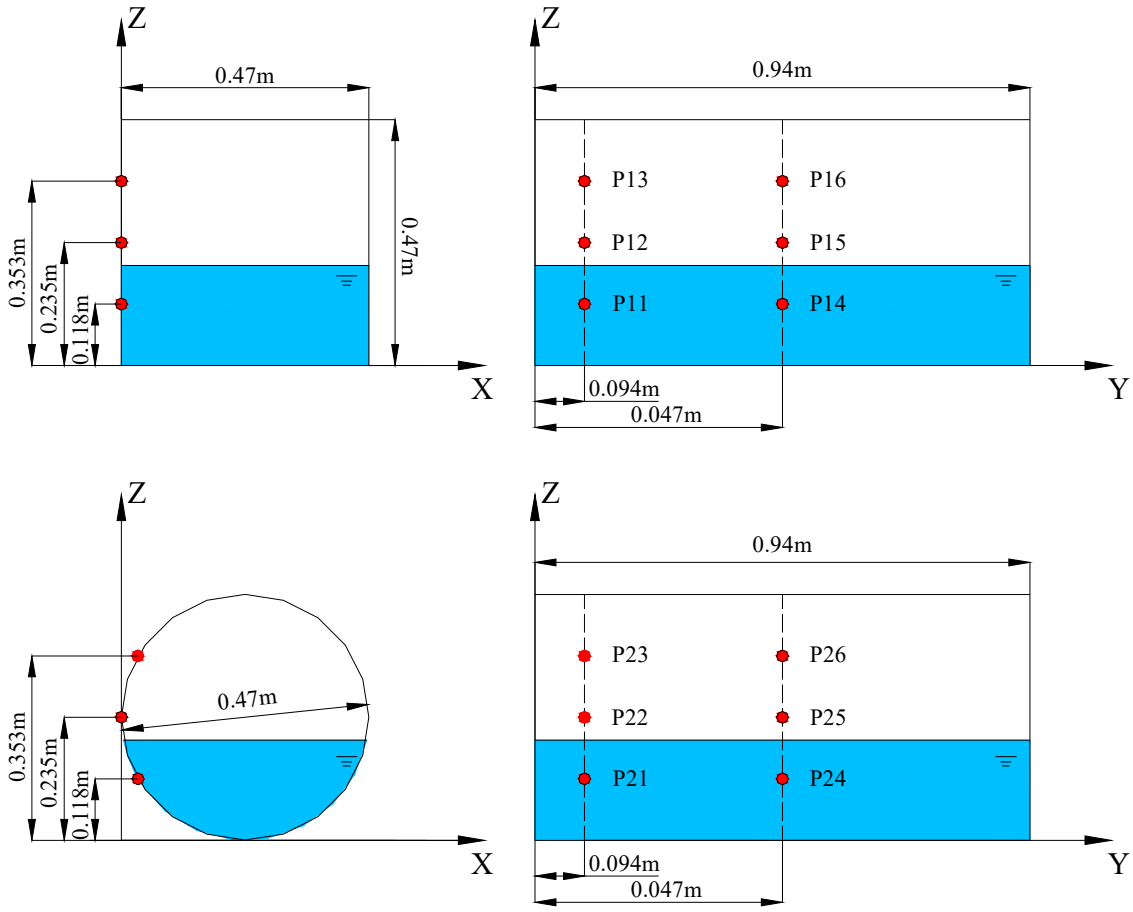

Figure 2. The sketch of numerical models

Six pressure probes are arranged on walls of both tanks to measure the time history of pressure and their specific locations are listed in Table 1.

Table 1 Arrangements of pressure probe

rectangular	X/m	Y/m	Z/m	cylinder	X/m	Y/m	Z/m
P11	0	0.094	0.118	P21	0.0315	0.094	0.118
P12	0	0.094	0.235	P22	0	0.094	0.235
P13	0	0.094	0.353	P23	0.0781	0.094	0.353
P14	0	0.470	0.118	P24	0.0315	0.470	0.118
P15	0	0.470	0.235	P25	0	0.470	0.235
P16	0	0.470	0.353	P26	0.0781	0.470	0.353

Verification

The accuracy of MLParticle-SJTU solver to simulate sloshing in rectangular tank has been validated in previous work. In this sub-section, the convergence verification of particle distance is conducted and the time history of resultant force in the Z direction is compared with the experimental data (Kobayashi et al., 1986) and the reliability of the solver to simulate sloshing in cylindrical tank is confirmed. The initial depth of water (h) is 0.235 m, corresponding filling ratio is 50%. The tank is forced to sway with the frequency ($\omega = 7.536\,\mathrm{rad/s}$) and the amplitude ($A = 0.015\,\mathrm{m}$). The model with initial spacing sizes of 0.0045 m, 0.005 m and 0.006 m is simulated to check the convergence of numerical results. Fig.3 compares the present numerical results with the experimental results. It can be noticed that the results of models with different spatial resolutions all agree well with the experimental results， which shows the accuracy and stability of the solver. Considering the computational efficiency and the refinement of flow field, initial distance between fluid particles is set to 0.005 m for the following simulation in this paper.

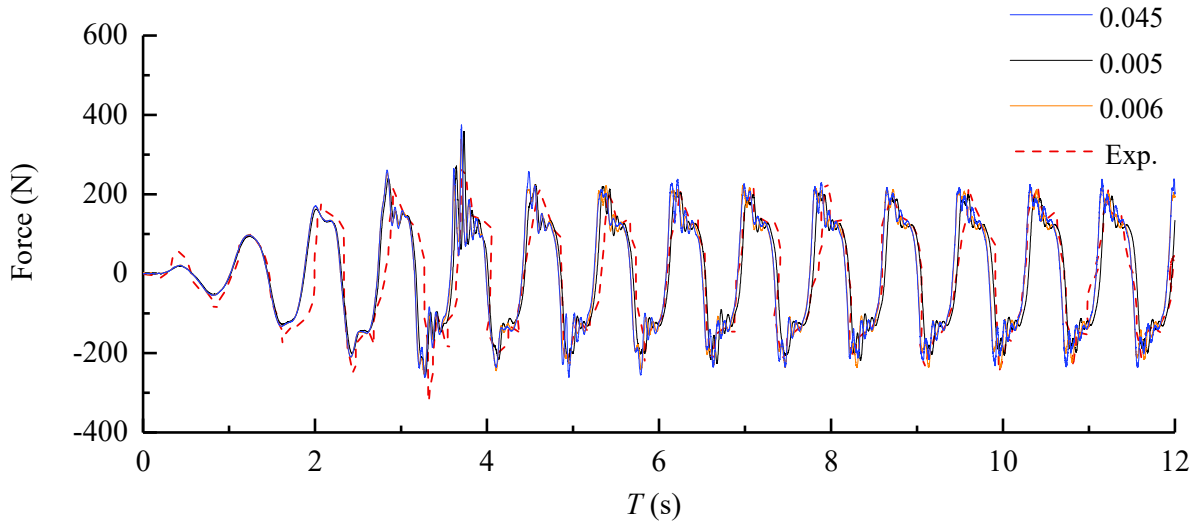

Figure 3. Time history of force in Z direction

Numerical conditions

In present paper, the sloshing in the cylindrical tank and the rectangular tank is compared at different filling ratios. The amplitude of motion is set to 0.015m. Considering the most extreme condition, tanks are excited at their respective natural frequencies. For rectangular tanks, the natural frequencies are calculated according to the formula (13). For cylindrical tanks, the natural frequencies are acquired according to the curve (Wiesche et al., 2008 [21]), which are presented in the Figure 4. Detailed parameters for numerical conditions are presented in Table 2.

$$\omega=\sqrt{\frac{g\pi}{L}\tanh\frac{\pi h}{L}} \tag{13}$$

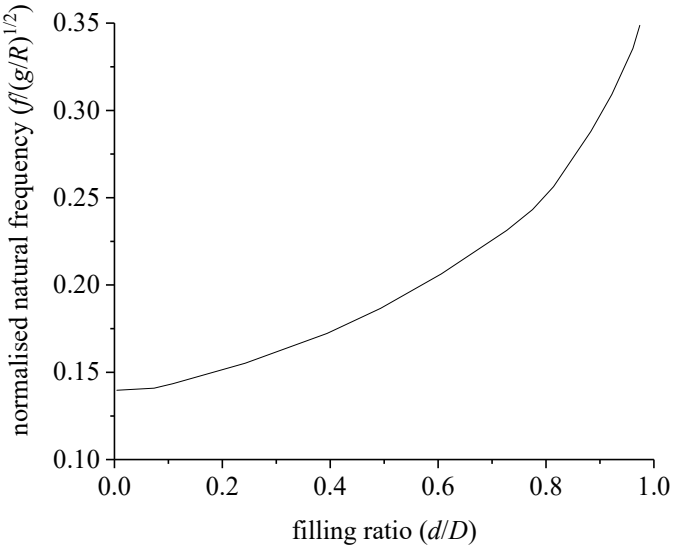

Figure 4. First transverse natural slosh frequency for horizontal cylindrical tanks(Wiesche et al. ,2008)

Table 2 Numerical conditions

rectangular tank			cylindrical tank		
filling ratio (h/H)	nature frequency ω_0 (rad/s)	particle number	filling ratio (h/H)	nature frequency ω_0 (rad/s)	particle number
0.25	6.558	709005	0.25	6.535	520060
0.5	7.755	1126389	0.5	7.805	939800
0.75	8.025	1491600	0.75	9.566	1321792

Numerical results

In this sub-section, there are some comparisons between cylindrical tank and rectangular tank presented.

Firstly, the tanks with low filling ratio (0.25) are compared. Figure 5 shows some snapshots of numerical flow field. The 3D effect in rectangular tank is more obvious than cylindrical tank's and a jumping phenomenon can be observed in rectangular tank. Besides, it can be noticed that slamming in rectangular tank is asymmetric. When the fluid flows to the left wall, the fluid in the middle of the wall is faster than that on both sides, impacting the roof of the tank. When the fluid flows to the right wall, the fluid on both sides of the wall is faster than that in the middle, reaching the higher position of the wall. The pressure time histories measured at different probes in the same tank are shown as Figure 6. For rectangular tank, the peak pressures and phases measured at P11 and P14 are very different, which indicates that traveling waves are generated along the longitudinal direction. For cylindrical tank, the peak pressures measured at P21 and P24 are slightly different and the pressure time histories are similar in general, which indicates that the waves traveling along the longitudinal direction are small and their influence to transverse sloshing is limited. In addition, the pressure time histories measured at different probes in different tanks are compared, as shown in Figure 7. The peak values of pressure measured at P14 and P24 are very close and the double pressure peaks can be observed at both probes when the waves in longitudinal direction haven't formed. Due to interaction of transverse sloshing mode and longitude sloshing mode, one of pressure peak disappears. There is a radian on the cylindrical wall and the momentum will be changed as fluid climb along the wall, so the peak values of pressure measured at P15 are generally higher than those measured at P25. However, the last few peak values of pressure at P15 are higher than those at P25 because of 3D effect. The probe P26 arranged at the highest position hardly detect the pressure, which indicates that the fluid have detached the wall before it arrived at the probe.

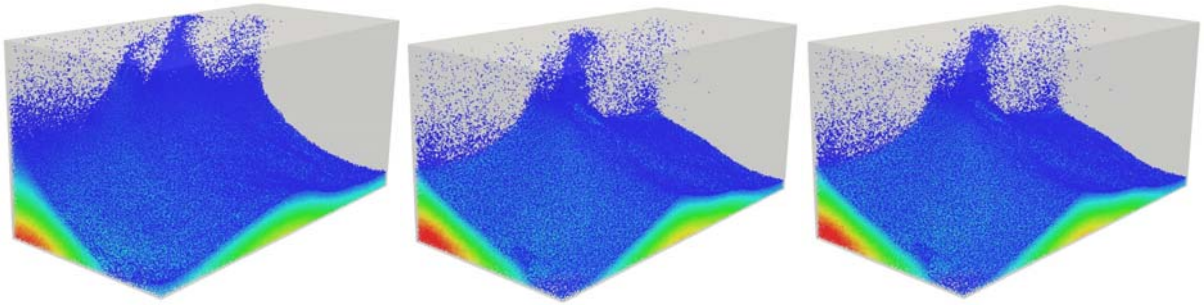

(a1) 16.35s (a2) 16.47s (a3) 16.59s

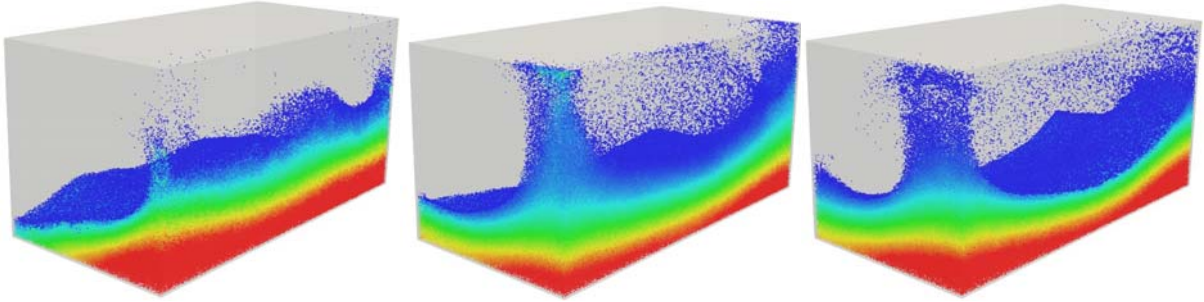

(a4) 16.71s (a5) 16.83s (a6) 16.95s

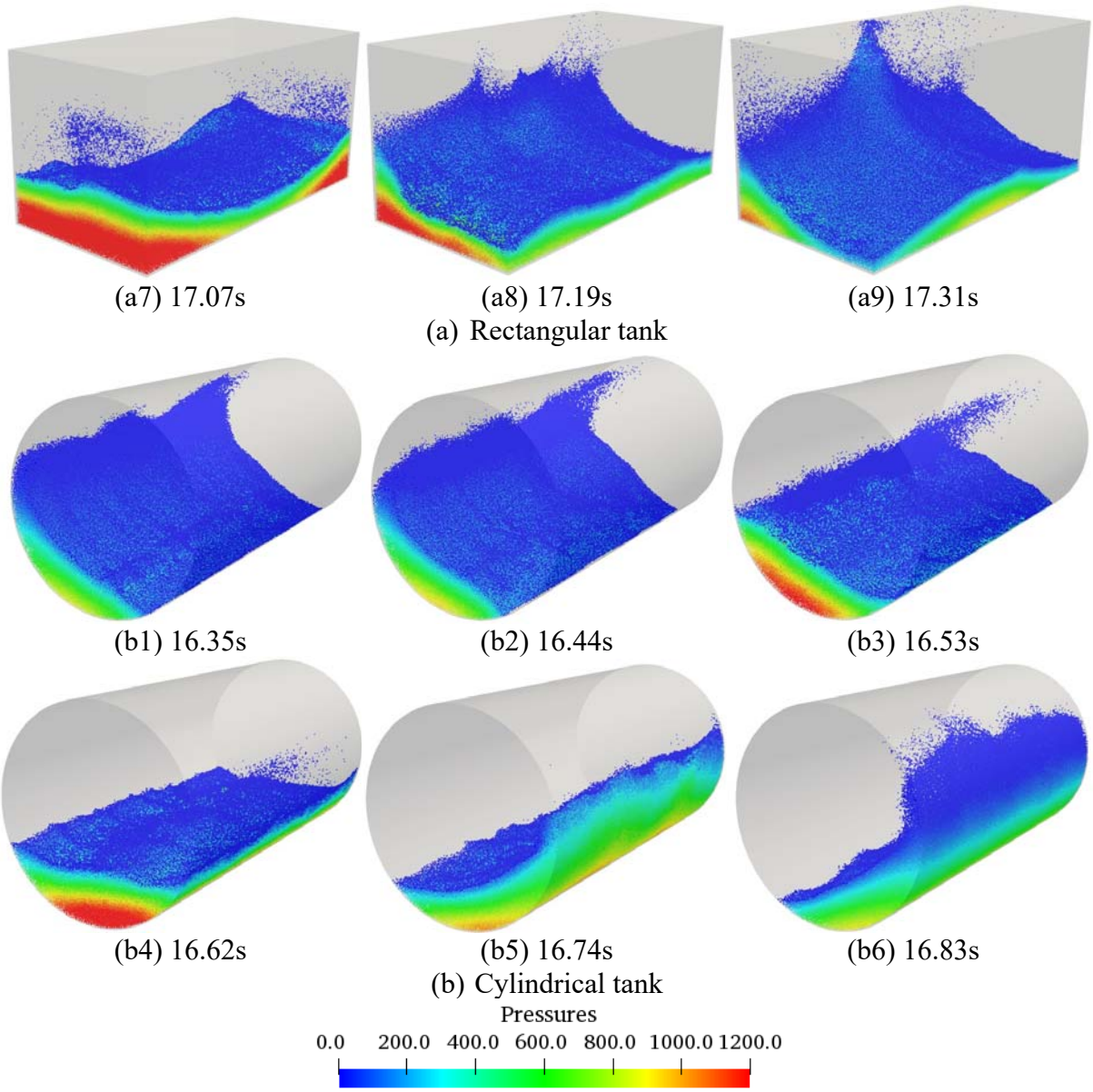

Figure 5. The flow fields in rectangular tank and cylindrical tank(h/H=0.25)

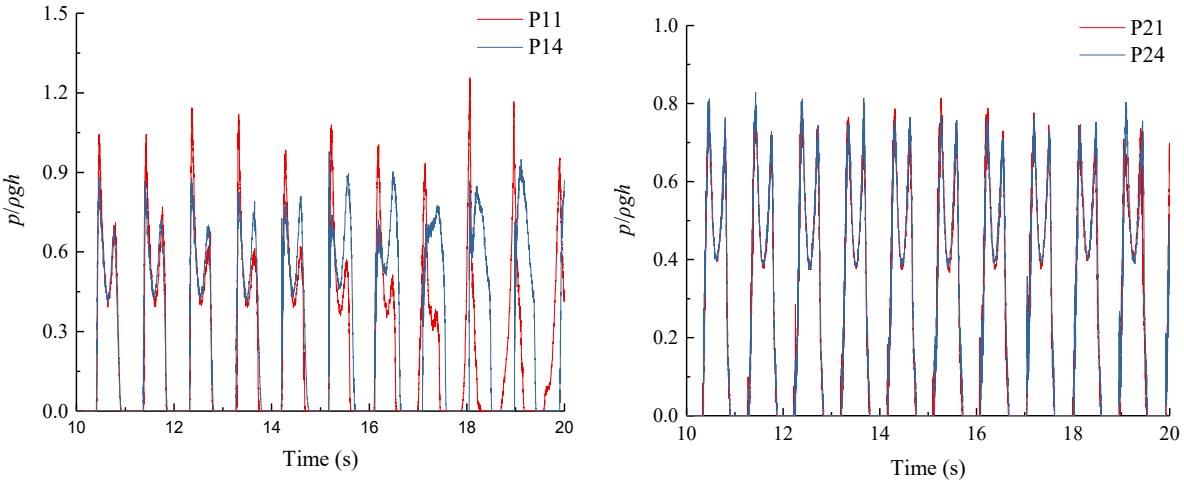

(a) P11 and P14 (b) P21 and P24

Figure 6. Time history of pressures measured at different probes in the same tank(*h*/*H*=0.25, Left: rectangular tank, Right: cylindrical tank)

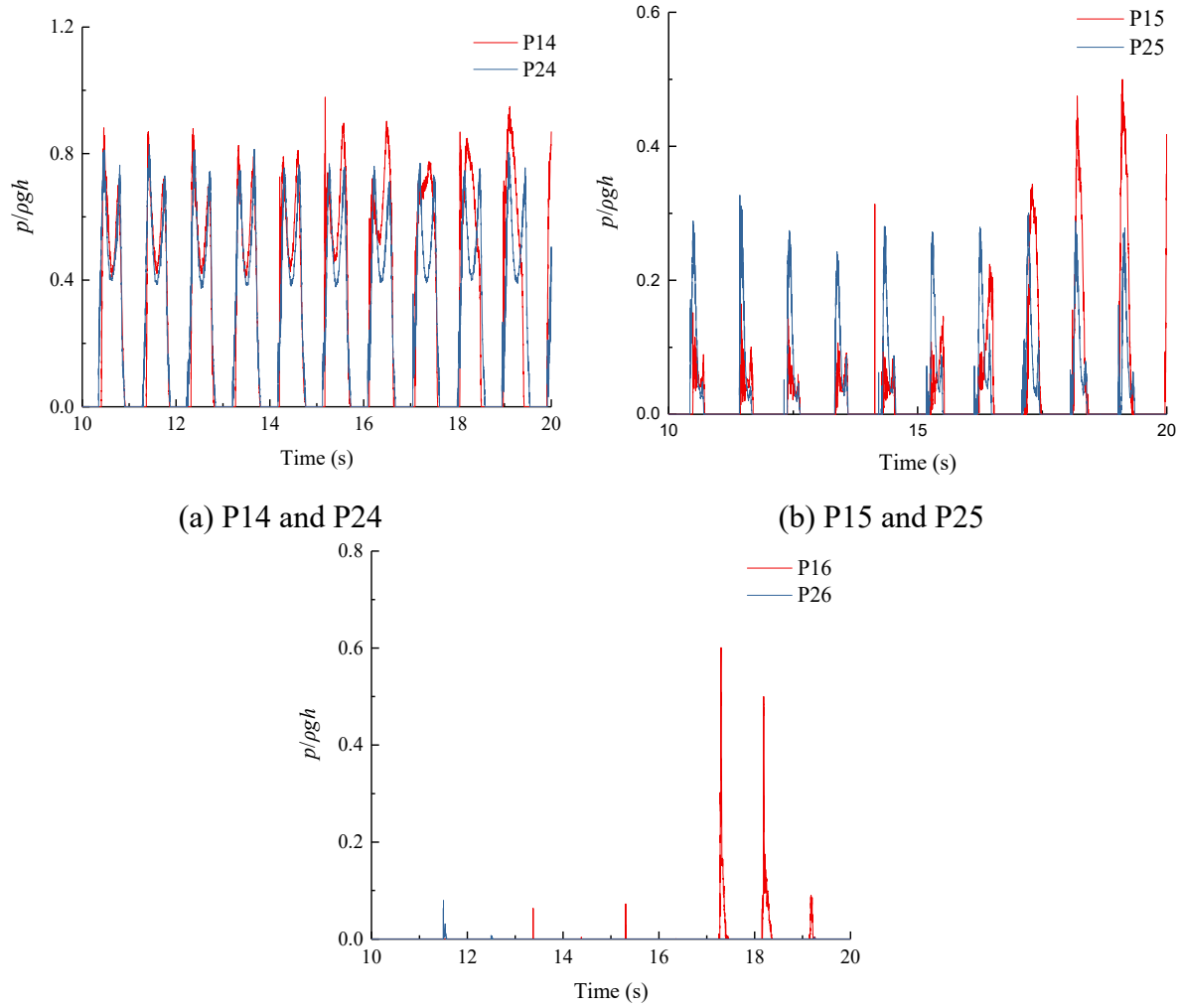

(a) P14 and P24 (b) P15 and P25

(c) P16 and P26

Figure 7. Time history of pressures measured at different probes in different tanks(*h*/*H*=0.25, red line: rectangular tank, blue line: cylindrical tank)

Secondly, the tanks with the filling ratio of 0.5 are compared. Figure 8 shows some snapshots of numerical flow field and Figure 9 shows the comparisons of pressure time histories measured at different probes in the same tank. The conclusions drawn from this simulation are similar to those obtained from simulation with low filling ratio. Figure 10 shows the comparisons of pressure time histories measured by different probes in different tanks. Before 15s，the 3D effect is at initial stage and peak values of pressure measured at probes of cylindrical tank are all slightly higher than those measured at corresponding probes of rectangular tank. After 15s，the 3D effect is at mature stage and the peak values of pressure measured by cylindrical tank probes all far less than those measured at corresponding probes in the rectangular tank. Besides, it can be noticed that time histories of pressure measured in rectangular tank is more randomness than those measured in cylindrical tank.

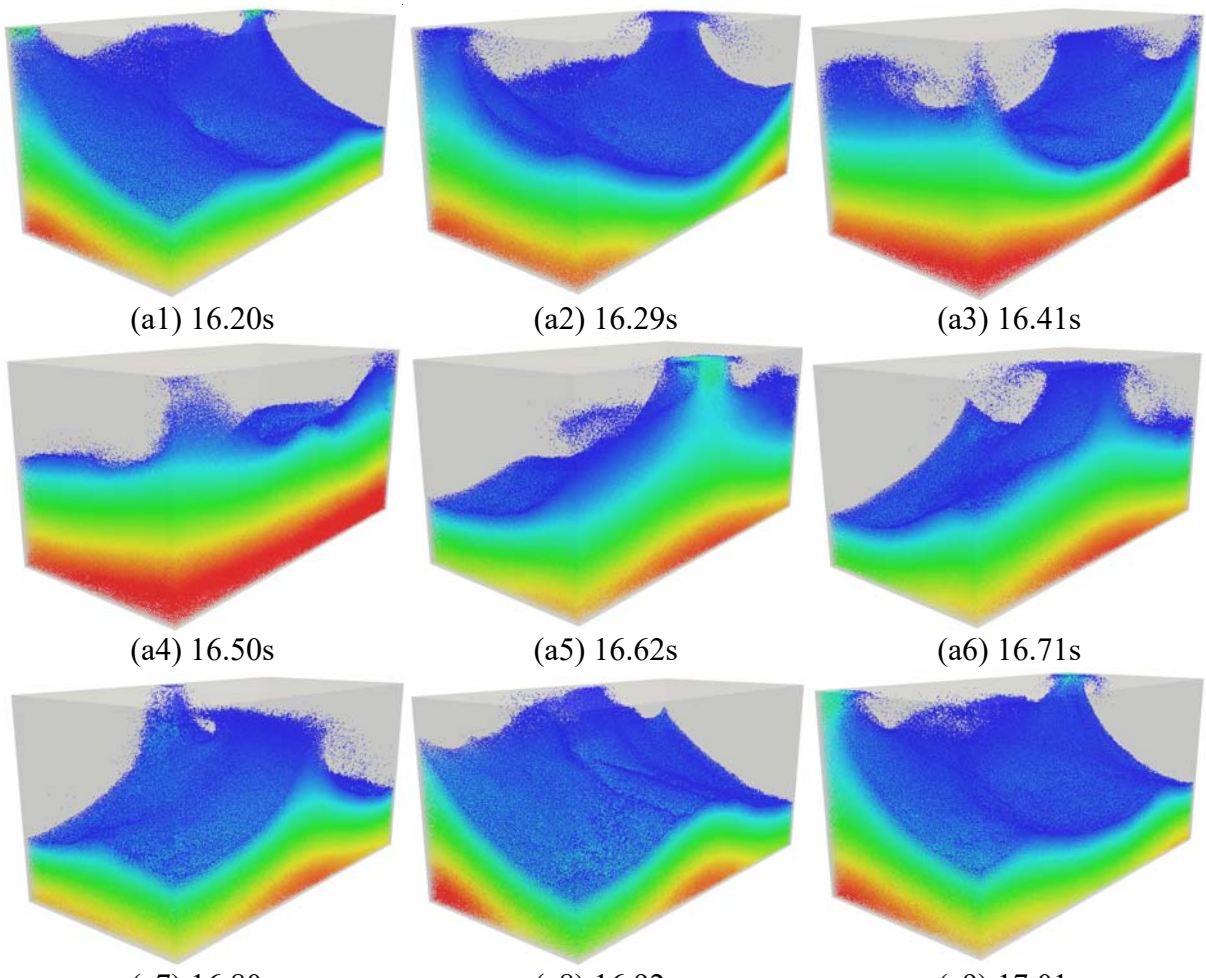

(a1) 16.20s (a2) 16.29s (a3) 16.41s

(a4) 16.50s (a5) 16.62s (a6) 16.71s

(a7) 16.80s (a8) 16.92s (a9) 17.01s

(a) Rectangular tank

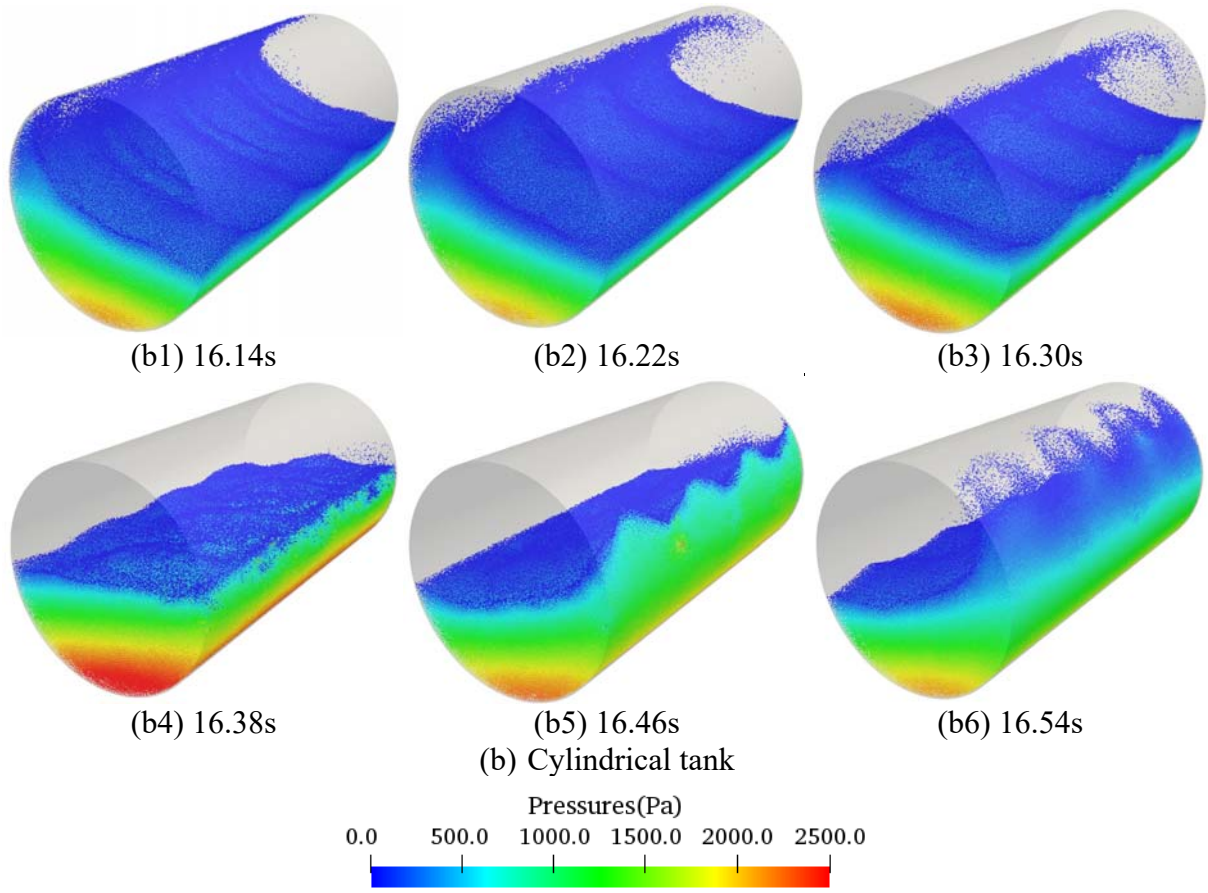

Figure 8. The flow fields in rectangular tank and cylindrical tank (*h*/*H*=0. 5)

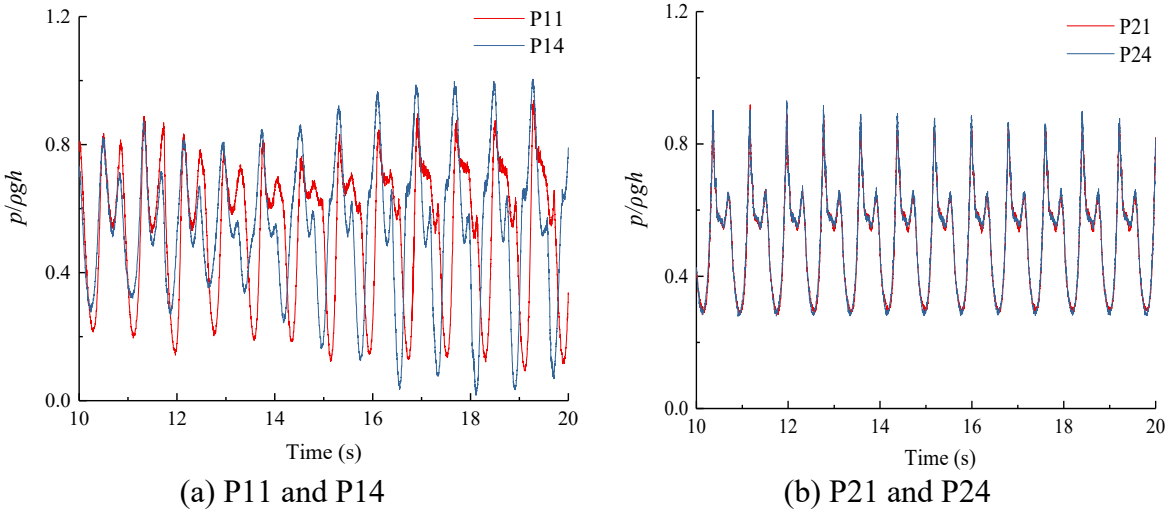

(a) P11 and P14 (b) P21 and P24

Figure 9. Time history of pressures measured at different probes in the same tank(*h*/*H*=0.5, Left: rectangular tank, Right: cylindrical tank)

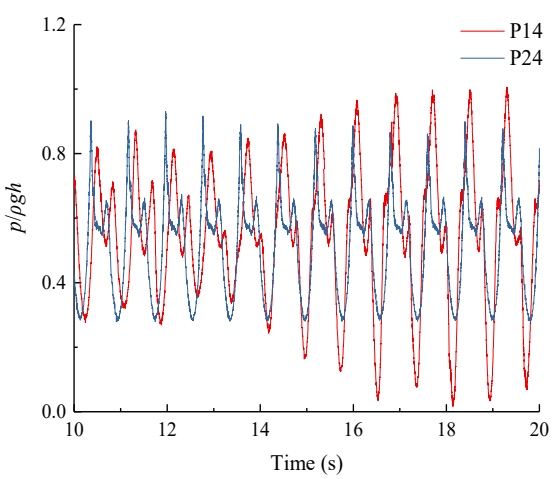

(a) P14 and P24

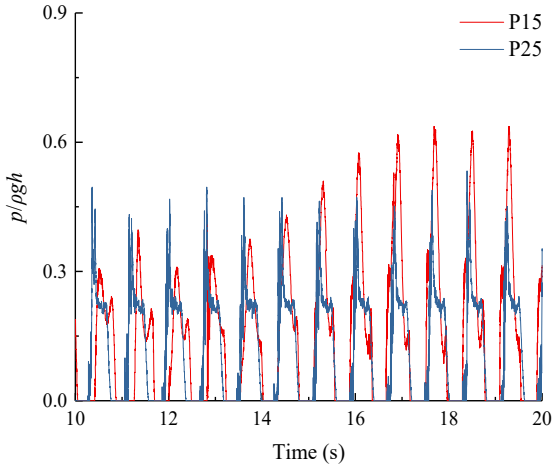

(b) P15 and P25

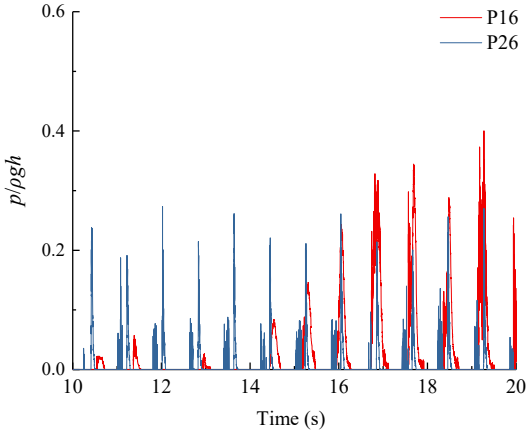

(c) P16 and P26

Figure 10. Time history of pressures measured at different probes in different tanks(*h*/*H*=0.5, red line: rectangular tank, blue line: cylindrical tank)

Finally, the tanks with high filling ratio (0.75) are compared. There is no obvious 3D effect observed in either type of tank, as shown in Figure 11 and Figure 12. This is because the roof plays a role as a horizontal buffer and prevents the further development of 3D effect. Figure 13 shows the comparisons of pressure time histories measured at different probes in different tanks. It is noticed that the pressure peak of cylindrical tank is higher than rectangular tank's. Besides, two successive peaks of pressure can be observed at each probe and the difference between those two peaks of cylindrical tank is much greater than rectangular tank's. Most of water will flow through the roof and fall to the fee surface in cylindrical tank. However, much water will go back along the wall in rectangular bank.

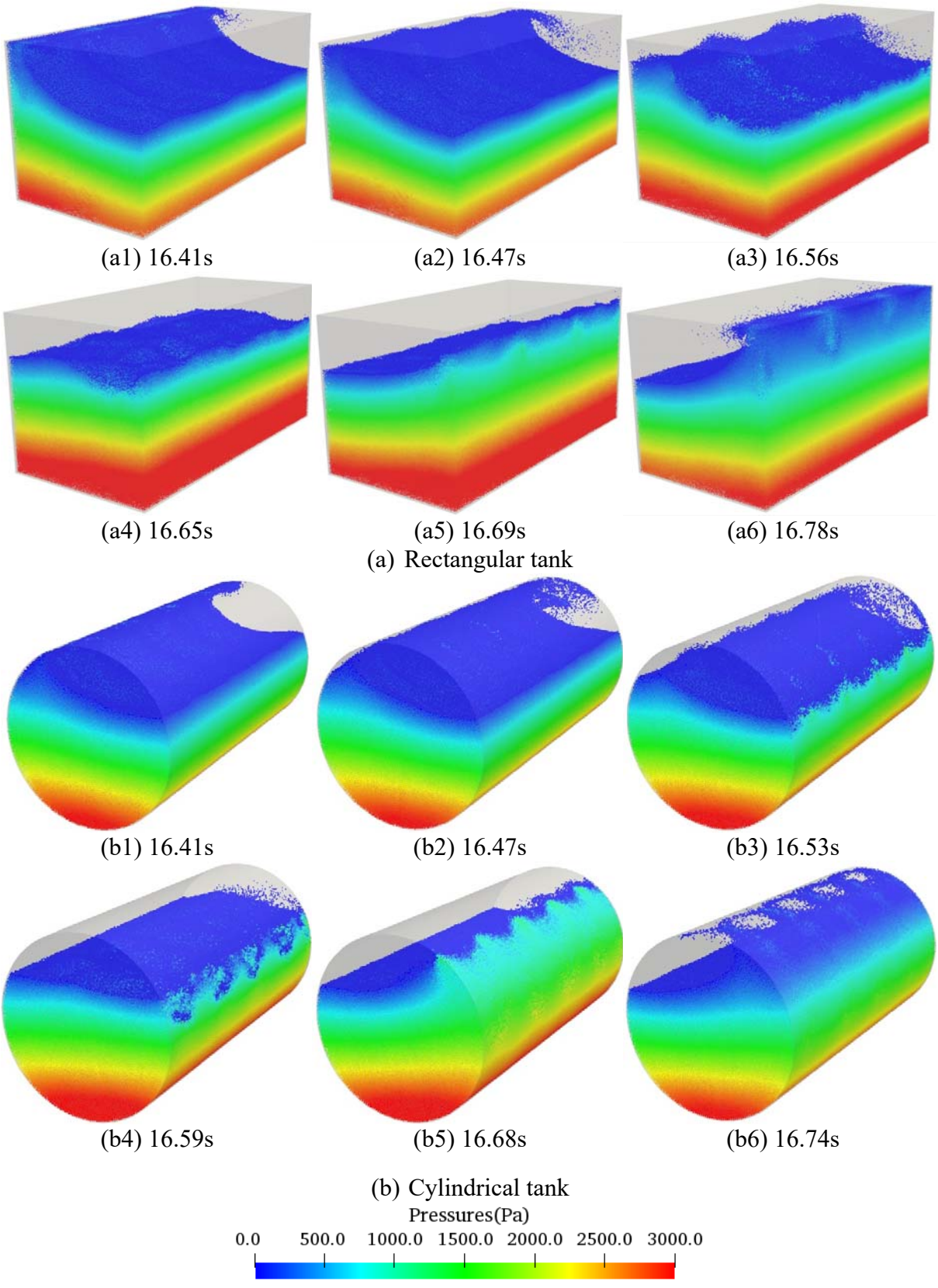

Figure 11. The flow fields in rectangular tank and cylindrical tank (*h*/*H*=0. 75)

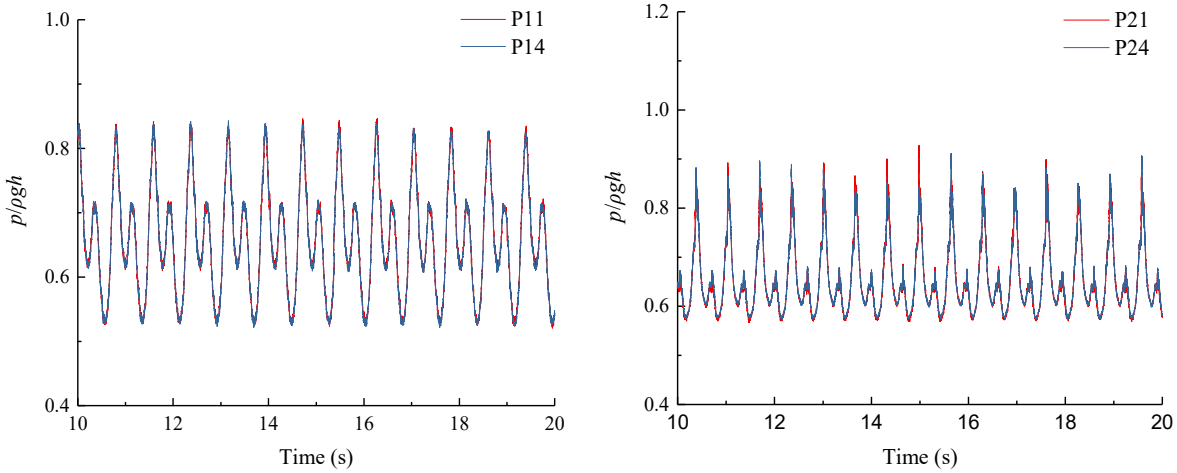

(a) P11 and P14 (b) P21 and P24

Figure 12. Time history of pressures measured at different probes in the same tank(*h*/*H*=0.75, Left: rectangular tank, Right: cylindrical tank)

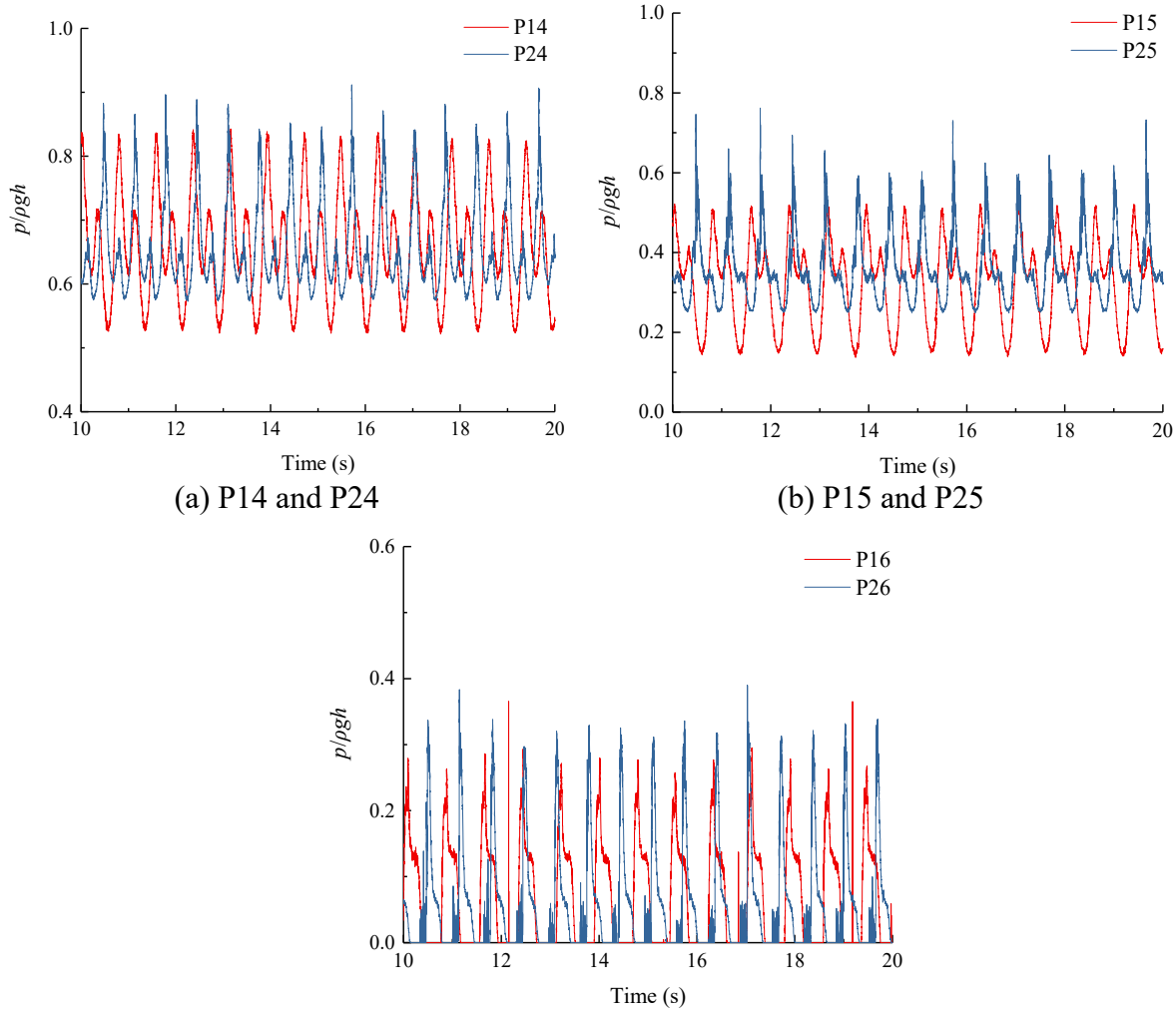

(a) P14 and P24 (b) P15 and P25

(d) P16 and P26

Figure 13. Time history of pressures measured at different probes in different tanks(*h*/*H*=0.75, red line: rectangular tank, blue line: cylindrical tank)

Conclusions

In this paper, the MLParticle-SJTU solver based on modified MPS is employed to investigate difference of sloshing in rectangular tank and cylindrical tank. The convergence verification is conducted to confirm the reliability of the solver. The comparison of pressure measured by different probes and the numerical flow field are presented. Based on the results of simulations, the following conclusions can be summarized:

- The 3D effect observed in rectangular tank with filling ratio of 0.25 and 0.5 is more obvious than that in cylindrical tank and a jumping phenomenon can be observed. The same conclusion can be drawn throw the comparison of pressure time history measured at different probes in the same tank at the same height. The peaks and phases are different in rectangular tank while those show a good agreement in cylindrical tank.
- When the 3D effect has not formed, the pressure peaks measured in rectangular tank is less than or close to those measured by corresponding probes in cylindrical tank. As the 3D effect become more severe, the pressure peaks measured in rectangular tank is far higher than those in cylindrical tank.
- With filling ratio of 0.75，The difference of two successive pressure peak in cylindrical tank is much greater than those in rectangular tank. Because, after slamming the roof, most of water will flow through the roof and fall to the fee surface in cylindrical tank while much water will go back along the wall in rectangular bank.

Acknowledgements

This work is supported by the National Natural Science Foundation of China (51879159, 51490675, 11432009, 51579145), Chang Jiang Scholars Program (T2014099), Shanghai Excellent Academic Leaders Program (17XD1402300), Program for Professor of Special Appointment (Eastern Scholar) at Shanghai Institutions of Higher Learning (2013022), Innovative Special Project of Numerical Tank of Ministry of Industry and Information Technology of China (2016-23/09) and Lloyd's Register Foundation for doctoral student, to which the authors are most grateful.

References

[1] Faltinsen, O. M. (1978) A numerical nonlinear method of sloshing in tanks with two-dimensional flow, *Journal of Ship Research* **22**(3), 193-202.

[2] Milkelis, N. E. and Robinson, D. W. (1985) Sloshing in arbitrary shaped tanks, *Journal of the Society of the Naval Architects of Japan* **158**, 246-255.

[3] Sussman, M., Fatemi, E., Smereka, P., et al. (1998) An improved level set method for incompressible two-phase flows, *Computers & Fluids* **27**(5), 663-680.

[4] Liu, Z., and Huang, Y. (1994) A new method for large amplitude sloshing problems, *Journal of Sound and Vibration* **175**(2), 185-195.

[5] Kim, Y., Nam, B. W., Kim, D. W. and Kim, Y. S. (2007) Study on coupling effects of ship motion and sloshing, *Ocean Engineering* **34**(16), 2176-2187.

[6] Belakroum, R., Kadja, M., Mai, T.H., Maalouf, C. (2010) An efficient passive technique for reducing sloshing in rectangular tanks partially filled with liquid, *Mechanics Research Communications* **37**(3), 341-346.

[7] Zhuang, Y. and Wan, D. C. (2017) Numerical study on ship motion fully coupled with LNG tank sloshing in CFD method, *International Journal of Computational Methods*, 1840022.

[8] Iglesias, A. S., Rojas, L. P. and Rodriguez, R. Z. (2004) Simulation of anti-roll tanks and sloshing type problems with smoothed particle hydrodynamics, *Ocean Engineering* **31**(8), 1169-1192.

[9] Iglesias, A. S., Delorme, L., Rojas L. P., et al. (2006) Liquid moment amplitude assessment in sloshing type problems with smooth particle hydrodynamics, *Ocean Engineering* **33**(11). 1462-1484.

[10] Delorme, L., et al. (2009) A set of canonical problems in sloshing, Part I: Pressure field in forced roll—comparison between experimental results and SPH, *Ocean Engineering* **36**(2), 168-178.

[11] Zhang, Y. X. and Wan, D. C. (2012) Apply MPS method to simulate liquid sloshing in LNG tank, *Phytotherapy Research* **29**(12), 1843–1857.

[12] Koh, C. G., Luo, M., Gao, M., et al. (2013) Modelling of liquid sloshing with constrained floating baffle, *Computers and Structures* **122**, 270-279.

[13] Zhang, Y. L. and Wan, D. C. (2017) MPS-FEM coupled method for sloshing flows in an elastic tank, *Ocean Engineering* **152**, 416-427.

[14] Chen, X., Zhang Y. L. and Wan, D. C. (2017) *GPU acceleration of MPS for three-dimensional sloshing*, Proceedings of the 8th International Conference on Computational Methods (ICCM2017), Guilin, Guangxi, China.

[15] Wen, X. and Wan, D. C. (2018) *Numerical Simulation of Three-Layer-Liquid Sloshing by Multiphase MPS Method*, the ASME 2018 37th International Conference on Ocean, Offshore and Arctic Engineering, Madrid, Spain.

[16] Koshizuka, S. and Oka, Y. (1996) Moving-Particle Semi-Implicit Method for Fragmentation of Incompressible Fluid, *Nuclear Science and Engineering* **123**(3), 421-434.

[17] Zhang, Y. X., Wan, D. C. and Hino, T. (2014) Comparative study of MPS method and level-set method for sloshing flows, *Journal of hydrodynamics* **26**(4), 577–585.

[18] Tanaka, M. and Masunaga, T. (2010) Stabilization and smoothing of pressure in MPS method by quasi-compressibility, *Journal of Computational Physics* **229**(11), 4279-4290.

[19] Zhang, Y. X. and Wan, D. C. (2012) *Apply MPS method to simulate liquid sloshing in LNG tank*, Proceedings of the 22nd International Offshore and Polar Engineering Conference, Rhodes, Greece.

[20] Kabayashi, N., Mieda, T. and Shibata, H. (1989) A Study of the Liquid Slosh Response in Horizontal Cylindrical Tanks, *Journal of Pressure Vessel Technology* **111**, 32-38.

[21] Wiesche and Stefan, A. D. (2008) Sloshing dynamics of a viscous liquid in a spinning horizontal cylindrical tank, *Aerospace Science and Technology* **12**(6), 448-456.